Liquid-liquid critical point in a simple analytical model of water

Tomaz Urbic*
Faculty of Chemistry and Chemical Technology, University of Ljubljana, Vecna Pot 113, 1000 Lubljana, Slovenia
(Received 16 August 2016; published 21 October 2016)

A statistical model for a simple three-dimensional Mercedes-Benz model of water was used to study phase diagrams. This model on a simple level describes the thermal and volumetric properties of waterlike molecules. A molecule is presented as a soft sphere with four directions in which hydrogen bonds can be formed. Two neighboring waters can interact through a van der Waals interaction or an orientation-dependent hydrogen-bonding interaction. For pure water, we explored properties such as molar volume, density, heat capacity, thermal expansion coefficient, and isothermal compressibility and found that the volumetric and thermal properties follow the same trends with temperature as in real water and are in good general agreement with Monte Carlo simulations. The model exhibits also two critical points for liquid-gas transition and transition between low-density and high-density fluid. Coexistence curves and a Widom line for the maximum and minimum in thermal expansion coefficient divides the phase space of the model into three parts: in one part we have gas region, in the second a high-density liquid, and the third region contains low-density liquid.

DOI: 10.1103/PhysRevE.94.042126

I. INTRODUCTION

The structure and thermodynamics of water and aqueous solutions are of great importance for chemistry and biology. Water molecules have a simple formula (H_2O), but it is a highly complex liquid. It has many anomalous properties due to the ability to form intermolecular hydrogen bonds. It is believed that these anomalies are related to the hypothetical second critical point between two liquid phases in a supercooled region [1]. This critical point was first discovered by computer simulations of the ST2 water model [2]. Much of the subsequent research was focused on proving or disproving the existence of liquid-liquid critical point (LLCP) and results to this day remain mixed [3–11]. Studies of water in ST2 as well as other models continue to support the LLCP hypothesis, but there is limited experimental evidence to back these claims up because the supposed LLCP is well below the homogenous nucleation temperature of water [12–14]. The anomalous properties of water and the possibility of liquid-liquid phase transition can be explained if water is viewed as a mixture of two interconvertible organizations of hydrogen bonds whose ratio is controlled by thermodynamic equilibrium [8,15–17]. The two-scale models have often been used as a way of explaining the thermodynamic and dynamic anomalies of liquid water. These models separate states of water into two different groups, one corresponding to low-energy low-entropy configurations and the other to high-energy high-entropy configurations. In these models water properties are modeled as a mixture of two different liquids. There exist also models which are extensions of the van der Waals equation with two microscopic states: hydrogen-bonded states (low-density water) and van der Waals states (high-density water) like the model by Poole *et al.* [18]. There is another group of lattice models [19,20] where water is presented as a lattice fluid in which bond formation depends strongly on molecular orientations and local density. These models are able to qualitatively reproduce the known thermodynamic behavior of water, including the behavior of supercooled water, and describe how the predictions of lattice-gas models are relevant to understanding liquid and amorphous solid water, but it is more difficult to use them for description of solvation effects. Tanaka [21,22] has a simple model of water that focuses on medium-range ordering in water. He introduces an additional bond order parameter next to a density order parameter. In the model he recognizes that in any liquid locally favored structures with low configurational entropy are formed in a sea of random, normal liquid structures with high configurational entropy. Anisimov and coworkers [3,6,8,9,15,16], on the other hand, describe water as a competition between an ideal entropy of mixing and a nonideal part of the Gibbs energy of mixing.

The aim of this work is to apply a statistical mechanical model we developed for a two-dimensional (2D) Mercedes-Benz model [23,24] to a three-dimensional (3D) Mercedes-Benz (MB) model of water. A previous version of the MB model dates back to the early 1970s [25–28]. Recently, a 3D Ben-Naim model was reinvented by Bizjak *et al.* [29,30] and Dias *et al.* [31,32] and studied using computer simulations [29–32] and integral equation theory [30]. Models are advantageous since they separate the hydrogen-bonding effect from others. The realistic models include many geometrical details and types of interactions, including electrostatic, hydrogen-bonding, and van der Waals interactions, which creates the difficulties in computational treatment and interpretation of obtained results. According to the 3D MB model, each water molecule is a Lennard–Jones sphere with four arms oriented tetrahedrally to mimic formation of hydrogen bonds. In a statistical mechanical model, which is based on Urbic and Dill's (UD) model [23] being directly descendant from a treatment of Truskett and Dill (TD), who developed a nearly analytical version of the 2D MB model [33,34], each water molecule interacts with its neighboring waters through a van der Waals interaction and an orientation-dependent interaction mimicking formation of hydrogen bonds.

II. THEORY

In the analytical theory, the structure of the liquid state is a perturbation from an underlying hexagonal (ice) lattice

*tomaz.urbic@fkkt.uni-lj.si

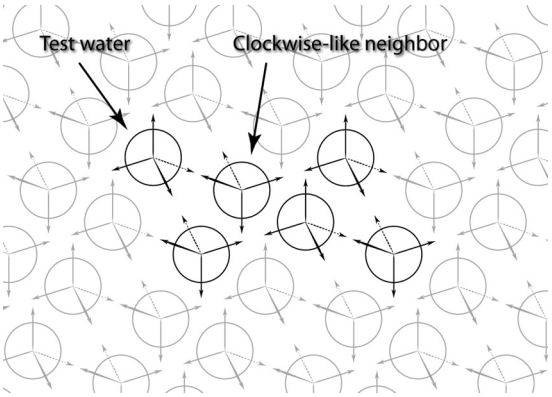

FIG. 1. One layer of the hexagon of the icelike lattice structure and a pair interaction used for bookkeeping to avoid triple counting.

(Fig. 1). Each water molecule is located close to one grid point which can be occupied by a single molecule. In the model, we focus on a single water molecule on the grid and its interactions with the neighbor molecule. Each molecule can be in one of three possible orientational states relative to its clockwiselike positioned neighbor on the lattice: (i) a hydrogen-bonded (HB) state, (ii) a van der Waals (vdW) state, or (iii) a nonbonded (NB) state where the two water molecules do not interact. This is presented in Fig. 2. First we compute the isothermal-isobaric statistical weights Δ_i of the states as a functions of temperature, pressure, and interaction energies [23,24]. In the HB state the test water molecule can point one of its four hydrogen-bonding arms at an angle θ to within $\pi/3$ of the center of its neighbor water. In this case it forms a hydrogen bond [24] (see Fig. 2) and the interaction energy of

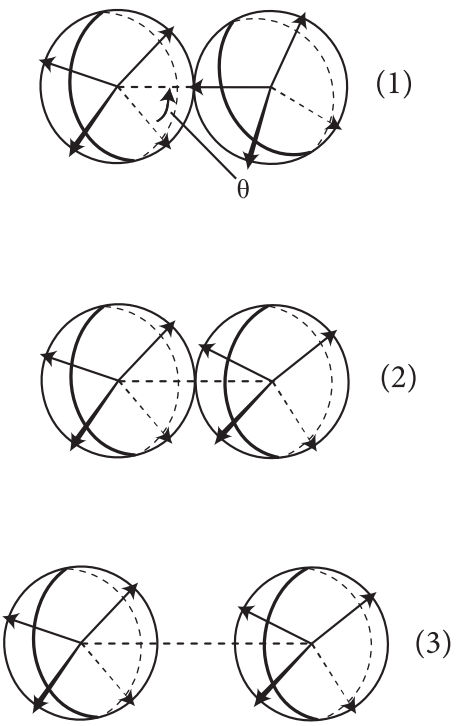

FIG. 2. The three states of the model: (1) hydrogen bonded, (2) van der Waals, and (3) nonbonded.

the test water with its neighbor is then

$$u_{HB}(\theta) = -\epsilon_{HB} + k_s(1+\cos\theta)^2, \quad 0 < \theta < \pi/3, \qquad (1)$$

where ϵ_{HB} is an HB energy constant of the maximal strength of an HB and k_s is the angular spring constant that describes the weakening of the hydrogen bond with angle. We treat this type of hydrogen bond as a weak bond [23], as it does not cooperate with neighboring hydrogen bonds. The isothermal-isobaric partition function Δ_{HB} of this state is calculated as an integral of this Boltzmann factor over all angles ϕ, θ, and ψ and over all the separations x, y, and z of the test molecule relative to its clockwise neighbor. In the vdW state, the test water molecule forms a contact with its clockwiselike positioned water, but there is no hydrogen bond. The energy of this state is

$$u_{LJ}(\theta) = -\epsilon_{LJ}, \quad 0 < \theta < \pi/3. \qquad (2)$$

The isothermal-isobaric partition function Δ_{LJ} of this state is obtained by the same procedure as for the HB state. In the last possible state, the test water molecule does not interact with its neighbors so the energy is

$$u_o(\theta) = 0. \qquad (3)$$

Upon obtaining the isobaric-isothermal ensemble Boltzmann weights of the three possible states of each water molecule and the partition function for a full hexagon of six waters can be written as

$$Q_1 = (\Delta_{HB} + \Delta_{LJ} + \Delta_o)^6, \qquad (4)$$

where the subscript 1 indicates a single hexagon. The total partition function for each hexagon, by taking into account also higher cooperativity in ice [23,24], is given by

$$Q_1 = (\Delta_{HB} + \Delta_{LJ} + \Delta_o)^6 - \Delta_{HB}^6 + \delta\Delta_s^6, \qquad (5)$$

where $\delta = \exp(-\beta\epsilon_c)$ is the Boltzmann factor for the cooperativity energy ϵ_c, which applies only when six water molecules all collect together into a full hexagonal cage. The terms on the right side of this expression simply replace the statistical weight for each weakly hydrogen-bonded full hexagonal cage with the statistical weight for a cooperative strongly hydrogen-bonded hexagonal cage. Δ_s is the Boltzmann factor for a cooperative hexagonal cage. It differs from Δ_{HB} only in the volume per molecule v_s instead of v_{HB} [23,24]. Now we combine the Boltzmann factors for the individual water molecules to get the partition function for the whole system of N particles; the population of different states can be calculated [23,24] and all the other thermodynamic properties from simple derivations of the partition function as described previously [23,24,33,34]. The attraction beyond pair is treated in the mean-field attractive level with energy [35] $-Na/v$ among hexagons, where a is the van der Waals dispersion parameter [23,33,34] and v is the average molar volume. The parameters needed for calculations can be obtained directly from the interaction pair potential between two $3d$ MB water particles ($\epsilon_{HB} = 1, r_{HB} = 1, k_s = 80, \epsilon_{HB} = 0.1, a = 0.045$, $\epsilon_c = 0.18$, and $\sigma_{LJ} = 0.7$) [29,30].

III. RESULTS AND DISCUSSION

Analytical theory has additional approximations compared to Monte Carlo simulations, which is why we first checked

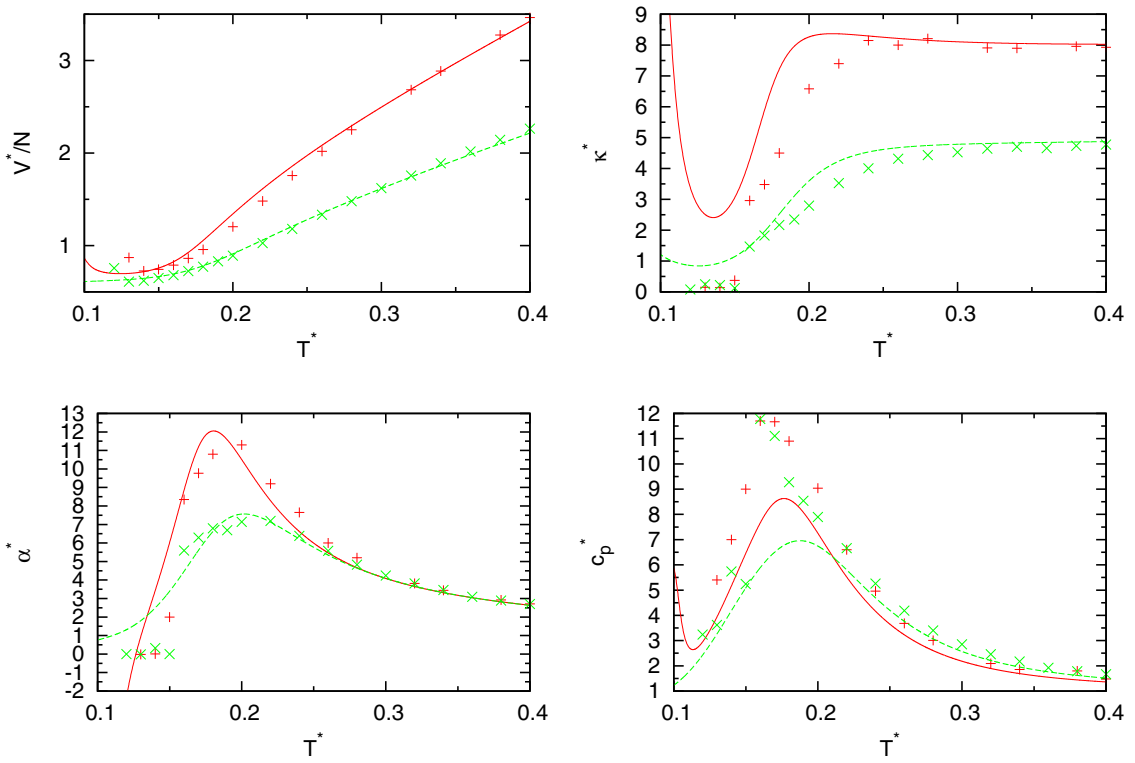

FIG. 3. Temperature dependence of the molar volume, thermal expansion coefficient, isothermal compressibility, and heat capacity for pressures $p^* = 0.19$ (green) and $p^* = 0.12$ (red) and comparison of analytical theory (lines) with results of computer simulations (symbols) [29,30].

the quality of the predictions of the analytical theory. We calculated the temperature dependence of the density, heat capacity, isothermal compressibility, and thermal expansion coefficient for reported pressures [29,30]. For a 3D MB model it was previously shown that the Mercedes-Benz water qualitatively correctly reproduces the anomalies of water [29,30] for these quantities. Analytical results are presented in dimensionless units, normalized to the strength of the optimal hydrogen bond ϵ_{HB} and hydrogen bond separation r_{HB} ($T^* = k_B T/\epsilon_{HB}$, $u^{ex*} = u^{ex}/\epsilon_{HB}$, $V^* = V/r_{HB}^3$, and $p^* = pr_{HB}^3/\epsilon_{HB}$). In Fig. 3 a comparison of predictions of the present theory (lines) for the molar volume V^*/N, the thermal expansion coefficient α^*, the isothermal compressibility κ_T^*, and the heat capacity C_p^* vs temperature to *NPT* Monte Carlo simulations [29,30] (symbols) of the 3D MB model with the same parameters is shown. The calculations of the theory were performed at a reduced pressure of $p^* = 0.12$ and 0.19. The theory is in good general agreement with the simulations, including the density maximum (minima in molar volume). The thermal expansion coefficient is negative at low temperatures, which is consistent with computer simulations and with experiments for water. The Monte Carlo simulations of MB water do not show an experimentally observed minimum in the isothermal compressibility versus temperature. On the other hand, the present theory predicts a minimum in κ_T^*. This is consistent with scattering experiments [36]. At low temperatures, our present model shows a drop in C_p^* as the temperature is reduced.

Being satisfied with the prediction of the model, we continue our research by calculating the density of 3D MB water as a function of temperature along isobars (up to $p^* = 0.25$) and determine critical points of the model. Results are shown in Fig. 4. In this pressure range, upon increase of temperature density increases, reaches a maximum, and then decreases. The 3D MB model exhibits two critical points: the liquid-gas critical point (C1) at $T_{C1}^* = 0.116\,6$, $p_{C1}^* = 0.011\,5$, $\rho_{C1}^* = 0.467$, and the liquid-liquid critical point (C2) at $T_{C2}^* = 0.077\,9$, $p_{C2}^* = 0.167$, and $\rho_{C2}^* = 1.295$. There exists also a region of pressures between both critical points where we have only one fluid phase, at higher pressures we have two liquid phases, and at lower pressures the liquid and the gas phases.

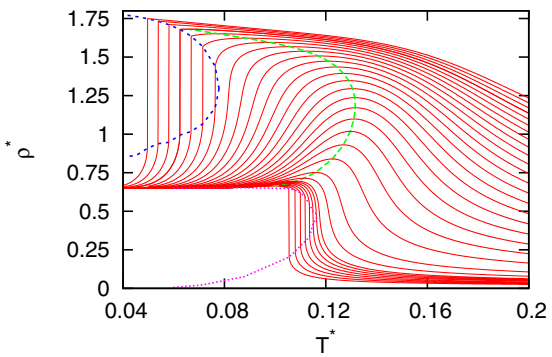

FIG. 4. Temperature dependence of the density for various pressures (red solid line), high-density liquid–low-density liquid coexistence line (green long-dashed line), liquid-gas density coexistence line (pink dotted line), and maximum densities (green dashed line).

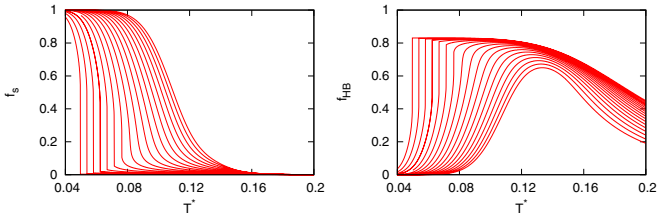

FIG. 5. Low-density fraction f_s and high-density fraction f_{HB} as a function of temperature for various isotherms ($p^* = 0.06$–0.23).

The model also gives us a chance to study what is happening with populations of different states. According to Mishima and Stanley, if the intermolecular potential of a pure fluid exhibits two minima, the interplay between the two indicates that a liquid-liquid separation may be present [12]. In our theory we have two states with different energies and volume, which is equivalent to having a potential with two minima. The initial 3D MB potential has a Lennard-Jones (LJ) minima and HB minima. There is also competition in the model between translation and orientational order. In Fig. 5 we plotted populations of low-density and high-density fractions as a function of temperature at different pressures. Upon heating of water cage structures of solid phase are converted by phase transition into closed-packed hydrogen bond structures of high-density phase or slowly change for pressures lower than critical pressure (C2). All this is in agreement with the prediction of the two-state thermodynamics in the model by Holten *et al.* [9], as well as for a two-state model for TIP4P/2005 water [37]. Experimental IR results [38] for structural change of confined water upon crossing the Widom line show same temperature dependence of the relative population of high-density amorphouslike and low-density amorphouslike water species, as predicted by our model for pressures outside the phase transition region.

Figure 6 contains the phase diagram of the noncrystalline phases of a 3D MB model of water. The phase diagram of a 3D MB fluid shows regions where at given pressure and temperature two coexisting phases are present separated by coexisting lines: gas and liquid by the gas-liquid coexisting line and two liquid phases by the liquid-liquid coexisting line. These lines terminate at the critical point. The model predicts a liquid-liquid coexistence curve with a negative derivative $\frac{dp}{dT}$, as predicted for real water [39]. It has been recently

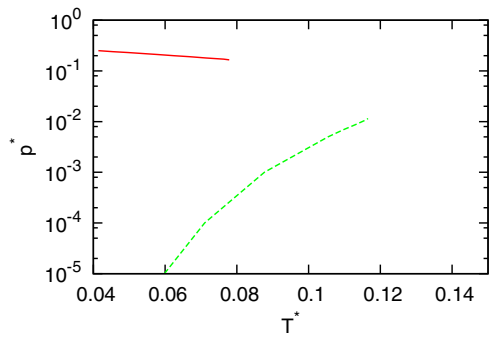

FIG. 6. Phase diagram of the noncrystalline phases of water. Red solid line is liquid-liquid and green dashed line liquid-gas coexistence line.

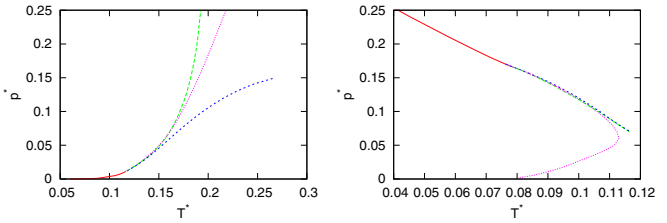

FIG. 7. Coexistence line (red solid line) with position of extremes of heat capacity (green long-dashed line), isothermal compressibility (blue dashed line), and thermal expansion coefficient (pink dotted line) for liquid-liquid (left) and liquid-gas (right) transition and supercritical region.

reported that for supercritical water there exist different regimes that are not separated by any first-order line of transition as in the subcritical region [40]. The two regions are separated by the so called Widom line that connects the maxima of the thermodynamic response functions upon approaching the critical point from the single supercritical phase. Figure 7 shows calculated coexistence lines for both phase transitions as well as maximums of heat capacity, isothermal compressibility, and thermal expansion coefficient (in case of C2 minima in thermal expansion coefficient) in the single-phase region after the critical point. All these curves are related to the Widom line. Starting from the critical point the curves first follow a similar path. In case of C1, the maxima of compressibility deviates from the other two lines at some distance from the critical point and later the other two lines also separate. For both critical points, lines for heat capacity and isothermal compressibility terminate while lines for thermal expansion coefficient continue and terminate only when bumping into the gas-liquid coexisting line and at zero temperature, like those observed for van der Waals gas [41]. In the framework of the van der Waals equation it has been possible to obtain exact analytical expressions for these lines in the region of a supercritical fluid and to determine how far from the critical point a single Widom line for different thermodynamic values may be established. Our model has limiting behavior for the van der Waals model [24] but can also predict two liquid phases. For the model coexistence lines and the curves of maxima and minima in the thermal expansion coefficient divide the phase space into three regions, as shown in Fig. 8. Each region contains one phase. In one part we have

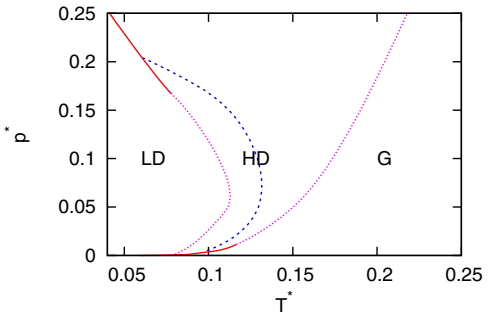

FIG. 8. Phase space of water model is split into three parts: LD- low-density liquidlike phase, HD- high-density liquidlike phase, and G- gaslike phase.

the gas region, in the second high-density liquid, and the third region contains low-density liquid.

IV. CONCLUSIONS

Summing up, we can conclude that in the analytical model for 3D MB water it has been possible to obtain analytical expressions for thermodynamic properties and a phase diagram including Widom lines in the regions of supercritical fluids. The 3D MB model has a similar noncrystalline phase diagram as real water, and Widom lines for the thermal expansion coefficient with coexistence curves divide the phase space into three regions, each containing its own fluid phase. It is expected that a system with richer internal freedom, meaning having more than two states, can have a richer phase space with even more divisions.

ACKNOWLEDGMENTS

T.U. is grateful for the support of the NIH (GM063592), the Slovenian Research Agency (P1 0103-0201, N1-0042), and the National Research, Development and Innovation Office of Hungary (SNN 116198).

[1] P. Gallo, K. Amann-Winkel, C. A. Angell, M. A. Anisimov, F. Caupin, C. Chakravarty, E. Lascaris, T. Loerting, A. Z. Panagiotopoulos, J. Russo, J. A. Sellberg, H. E. Stanley, H. Tanaka, C. Vega, L. Xu, and L. G. M. Pettersson, Chem. Rev. (Washington, DC, U. S.) **116**, 7463 (2016).
[2] P. H. Poole, F. Sciortino, U. Essmann, and H. Stanley, Nature (London) **360**, 324 (1992).
[3] J. W. Biddle, V. Holten, J. V. Sengers, and M. A. Anisimov, Phys. Rev. E **87**, 042302 (2013).
[4] L. Liu, S.-H. Chen, A. Faraone, C.-W. Yen, and C.-Y. Mou, Phys. Rev. Lett. **95**, 117802 (2005).
[5] H. E. Stanley, C. A. Angell, U. Essmann, M. Hemmati, P. H. Poole, and F. Sciortinoa, Phys. A (Amsterdam, Neth.) **205**, 122 (1994).
[6] D. A. Fuentevilla and M. A. Anisimov, Phys. Rev. Lett. **97**, 195702 (2006).
[7] D. T. Limmer and D. Chandler, J. Chem. Phys. **135**, 134503 (2011).
[8] V. Holten, C. E. Bertrand, M. A. Anisimov, and J. V. Sengers, J. Chem. Phys. **136**, 094507 (2012).
[9] D. T. Holten, V. Limmer, V. Molinero, and M. A. Anisimov, J. Chem. Phys. **138**, 174501 (2013).
[10] A. Nilsson and L. G. M. Pettersson, Chem. Phys. **389**, 1 (2011).
[11] Marco Aurelio A. Barbosa, E. Salcedo, and M. C. Barbosa, Phys. Rev. E **87**, 032303 (2013).
[12] O. Mishima and H. E. Stanley, Nature (London) **396**, 329 (1998).
[13] K.-I. Murata and H. Tanaka, Nat. Mater. **11**, 436 (2012).
[14] A. K. Soper and M. A. Ricci, Phys. Rev. Lett. **84**, 2881 (2000).
[15] C. E. Bertrand and M. A. Anisimov, J. Phys. Chem. B **115**, 14099 (2011).
[16] V. Holten and M. A. Anisimov, Sci. Rep. **2**, 713 (2012).
[17] L. Xu, S. V. Buldyrev, C. A. Angell, and H. E. Stanley, Phys. Rev. E **74**, 031108 (2006).
[18] P. H. Poole, F. Sciortino, T. Grande, H. E. Stanley, and C. A. Angell, Phys. Rev. Lett. **73**, 1632 (1994).
[19] C. J. Roberts and P. G. Debenedetti, J. Chem. Phys. **105**, 658 (1996).
[20] M. Pretti, C. Buzano, and E. De Stefanis, J. Chem. Phys. **131**, 224508 (2009).
[21] H. Tanaka, J. Chem. Phys. **112**, 799 (2000).
[22] H. Tanaka, Europhys. Lett. **50**, 340 (2000).
[23] T. Urbic and K. A. Dill, J. Chem. Phys. **132**, 224507 (2010).
[24] T. Urbic, Phys. Rev. E **85**, 061503 (2012).
[25] A. Ben-Naim, J. Chem. Phys. **54**, 3682 (1971).
[26] A. Ben-Naim, Mol. Phys. **24**, 705 (1972).
[27] A. Ben-Naim, *Water and Aqueous Solutions* (Plenum Press, New York, 1974).
[28] A. Ben-Naim, *Molecular Theory of Water and Aqueous Solutions*, 1st ed. (World Scientific, Singapore, 2009).
[29] A. Bizjak, T. Urbic, V. Vlachy, and K. A. Dill, Acta Chim. Slov. **54**, 532 (2007).
[30] A. Bizjak, T. Urbic, V. Vlachy, and K. A. Dill, J. Chem. Phys. **131**, 194504 (2009).
[31] C. L. Dias, T. Ala-Nissila, M. Grant, and M. Karttunen, J. Chem. Phys. **131**, 054505 (2009).
[32] C. L. Dias, T. Hynninen, T. Ala-Nissila, A. S. Foster, and M. Karttunen, J. Chem. Phys. **134**, 065106 (2011).
[33] T. M. Truskett and K. A. Dill, J. Chem. Phys. **117**, 5101 (2002).
[34] T. M. Truskett and K. A. Dill, J. Phys. Chem. B **106**, 11829 (2002).
[35] E. A. Jagla, J. Chem. Phys. **111**, 8980 (1999).
[36] C. Huang, K. T. Wikfeldt, T. Tokushimc, D. Nordlund, Y. Harada, U. Bergmann, M. Niebuhr, T. M. Weiss, Y. Horikawa, M. Leetmaa, M. P. Ljungberg, O. Takahashi, A. Lenz, L. Ojamae, A. P. Lyubartsev, S. Shin, L. G. M. Pettersson, and A. Nilsson, Proc. Natl. Acad. Sci. U.S.A. **106**, 15214 (2009).
[37] J. Russo and H. Tanaka, Nat. Commun. **5**, 3556 (2014).
[38] L. Xu, M. Mallamace, Z. Yan, F. W. Starr, S. V. Buldyrev, and H. E. Stanley, Nat. Phys. **5**, 565 (2009).
[39] K. Amann-Winkel, R. Böhmer, F. Fujara, C. Gainaru, B. Geil, and Thomas Loerting, Rev. Mod. Phys. **88**, 011002 (2016).
[40] P. Gallo, D. Corradini, and M. Rovere, Nat. Commun. **5**, 5806 (2014).
[41] V. V. Brazhkin and V. N. Ryzhov, J. Chem. Phys. **135**, 084503 (2011).